Genome Medicine

RESEARCH

Open Access

High density genomic surveillance and risk profiling of clinical *Listeria monocytogenes* subtypes in Germany

Sven Halbedel[1,2*†], Sabrina Wamp[1†], Raskit Lachmann[3], Alexandra Holzer[3], Ariane Pietzka[4], Werner Ruppitsch[5], Hendrik Wilking[3] and Antje Flieger[1*]

Abstract

Background Foodborne infections such as listeriosis caused by the bacterium *Listeria monocytogenes* represent a significant public health concern, particularly when outbreaks affect many individuals over prolonged time. Systematic collection of pathogen isolates from infected patients, whole genome sequencing (WGS) and phylogenetic analyses allow recognition and termination of outbreaks after source identification and risk profiling of abundant lineages.

Methods We here present a multi-dimensional analysis of > 1800 genome sequences from clinical *L. monocytogenes* isolates collected in Germany between 2018 and 2021. Different WGS-based subtyping methods were used to determine the population structure with its main phylogenetic sublineages as well as for identification of disease clusters. Clinical frequencies of materno-foetal and brain infections and in vitro infection experiments were used for risk profiling of the most abundant sublineages. These sublineages and large disease clusters were further characterised in terms of their genetic and epidemiological properties.

Results The collected isolates covered 62% of all notified cases and belonged to 188 infection clusters. Forty-two percent of these clusters were active for > 12 months, 60% generated cases cross-regionally, including 11 multinational clusters. Thirty-seven percent of the clusters were caused by sequence type (ST) ST6, ST8 and ST1 clones. ST1 was identified as hyper- and ST8, ST14, ST29 as well as ST155 as hypovirulent, while ST6 had average virulence potential. Inactivating mutations were found in several virulence and house-keeping genes, particularly in hypovirulent STs.

Conclusions Our work presents an in-depth analysis of the genomic characteristics of *L. monocytogenes* isolates that cause disease in Germany. It supports prioritisation of disease clusters for epidemiological investigations and reinforces the need to analyse the mechanisms underlying hyper- and hypovirulence.

Keywords Epidemiology, Outbreak, *inlF*, *flaR*, *clpP1*

†Sven Halbedel and Sabrina Wamp shared first authors.

*Correspondence:
Sven Halbedel
halbedels@rki.de
Antje Flieger
fliegera@rki.de
[1] FG11 Division of Enteropathogenic Bacteria and Legionella, Consultant Laboratory for Listeria, Robert Koch Institute, Burgstrasse 37, Wernigerode D-38855, Germany
[2] Institute for Medical Microbiology and Hospital Hygiene, Otto Von Guericke University Magdeburg, Leipziger Strasse 44, Magdeburg 39120, Germany
[3] FG35 – Division for Gastrointestinal Infections, Zoonoses and Tropical Infections, Robert Koch Institute, Seestrasse 10, Berlin 13353, Germany
[4] Austrian Agency for Health and Food Safety, Institute for Medical Microbiology and Hygiene, Beethovenstraße 6, Graz 8010, Austria
[5] Austrian Agency for Health and Food Safety, Institute for Medical Microbiology and Hygiene, Währingerstrasse 25a, Vienna 1090, Austria

Background

Listeriosis is a severe foodborne infection and may arise when food contaminated by the Gram-positive bacterium *Listeria monocytogenes* is consumed. Even though contamination of food items and consequently pathogen exposure is quite common [1], listeriosis generally occurs with low frequency, as reflected by the annual incidence of notified cases, which is in the range of 0.2–0.9 patients per 100,000 inhabitants in Europe and North America [2–4]. The immune system ensures efficient pathogen clearance after crossing of the gut epithelium [5], explaining low incidence of symptomatic cases in otherwise healthy individuals, where the infection may occur as asymptomatic or self-limiting gastroenteritis. However, invasive disease with manifestations such as septicaemia, neurolisteriosis or materno-foetal infections with high lethality may develop in immunocompromised patients or pregnant women and neonates, respectively [6]. Case fatality rates between 13 and 46% have been reported, depending on the length of the patient observation interval after infection or on the various disease manifestations [2, 7, 8]. Such rates are exceptionally high and generally not observed with other bacterial gastrointestinal pathogens [7, 9].

Prevention of *L. monocytogenes* food contamination is challenging, since the bacterium is ubiquitously found in many environmental habitats as well as in the digestive tract and lymphatic organs of productive livestock, leading to frequent contamination of raw materials or to cross-contamination in food processing plants [10–12]. Contamination control strategies are implemented at different levels of the food production chain and include optimisation of farming practices, improvement of product sanitation and storage conditions or implementation of cleaning and disinfection protocols in the production environment [13–15]. Moreover, European legislation has defined contamination limits for *L. monocytogenes* in ready-to-eat or infant food [16]. While all these measures doubtlessly help to keep listeriosis incidence low, large and protracted outbreaks of listeriosis regularly occur [17–19], highlighting the importance of disease surveillance systems for detection of clusters of epidemiologically linked cases over a prolonged time as a prerequisite to identify and inactivate the underlying source.

During the last years, several countries or supranational entities such as the European Union have established pathogen surveillance systems based on whole genome sequencing (WGS) of clinical and food isolates to allow cluster detection and assignment of food sources [20–24]. As a result, listeriosis outbreaks can now be detected in real time, enabling food authorities to implement countermeasures during ongoing outbreaks. WGS has also generated new insights in the relative contribution of different food vectors to the disease burden. We have shown this in a recent WGS-based surveillance study, where we estimated that ~ 30% of all German listeriosis cases with a known food source are related to consumption of salmon products [25]. Moreover, our knowledge on genomic diversity of *L. monocytogenes* strains, including the identification of hypo- and hypervirulent subtypes [26], their genetic determinants and the description of novel markers associated with stress, biocide and antibiotic resistance has strongly benefited from systematic genome sequencing [27–29].

In Germany, incidence of listeriosis steadily increased from 0.4/100,000 in 2011 to 0.9/100,000 in 2017, but was slightly lower in subsequent years [2]. This recent trend of declining case numbers coincided with the introduction of WGS in the German listeriosis surveillance system in 2018 [20], which had led to the detection and termination of large listeriosis outbreaks [18, 30–32]. We here present a high-density analysis of the genomic diversity and population structure of clinical *L. monocytogenes* strains isolated from listeriosis patients in Germany between 2018 and 2021 including a risk profiling of subtypes with international importance.

Methods

Bacterial strains and growth conditions

L. monocytogenes isolates obtained from human listeriosis cases in Germany were isolated by primary diagnostic labs and routinely sent to the Consultant Laboratory for *Listeria* at the Robert Koch Institute. All 1802 clinical *L. monocytogenes* strains used in this study are listed in Table S1. Samples were accompanied by sample submission forms that included basic information on the source of isolation as well as the disease manifestation. *L. monocytogenes* strains were routinely grown overnight (if not stated otherwise) in brain heart infusion (BHI) broth or on BHI agar plates at 37 °C. *L. monocytogenes* strains EGD-e (wild type IIc strain, ST35, CC9) [33] and its isogenic descendants BUG2214 (Δ*prfA*) [34], LMS3 (Δ*fliI*) [35], LMS250 (Δ*hly*) [36], LMJR156 (Δ*csbB*) [37], LMSW211 (Δ*flaR*, this work) as well as strain 10403S (wild type IIa strain, ST87, CC7) and its isogenic Δ*eslB* mutant [38] were included as controls in selected experiments.

Matching of isolates with notified cases

According to the German Protection Against Infection Act, laboratory confirmation of *L. monocytogenes* isolation or detection of nucleic acids from blood, cerebrospinal fluid or other usually sterile sites is notifiable to local health authorities and is electronically transmitted to the Robert Koch Institute (RKI). Case notification through the German notification system partially

includes information on disease manifestation (listeriosis of neonates, listeriosis of pregnant women, other forms of listeriosis) and symptoms (meningitis, sepsis, among others). These categories were combined with isolate identifiers and typing information through merging of isolates with notification cases.

Whole genome sequencing, molecular serogrouping, MLST and cgmlst

DNA was isolated by mechanical disruption using glass beads in a TissueLyser II bead mill (Qiagen, Hilden, Germany) [39] and quantified with a Qubit dsDNA BR (or HS) Assay kit and Qubit fluorometers (Invitrogen, Carlsbad, CA, USA). Libraries were prepared using the Nextera XT DNA Library Prep Kit and sequenced on MiSeq or NextSeq sequencers in 1×150 bp single end or 2×250 bp or 2×300 bp paired end mode. A SeqSphere (Ridom, Münster, Germany) script was used for read trimming and contig assembly with Velvet as the assembler. Molecular serogroups, seven locus multilocus sequence typing (MLST) sequence types (STs) and 1701 locus core genome MLST (cgMLST) complex types (CTs) were automatically extracted using SeqSphere [40]. Sequencing coverage was in the range of 17–184-fold (median: 59-fold). Samples in which at least 90% of the cgMLST alleles were called were considered samples with sufficient sequencing quality. cgMLST clusters and minimum spanning trees were calculated in SeqSphere in the "pairwise ignore missing values" mode. Phylogenetic trees were calculated in SeqSphere based on allele distance matrices as unrooted UPGMA tree in the "pairwise ignore missing values" mode from 1701 locus cgMLST data or as unrooted neighbour joining tree in the "missing values are an own category" mode from 7 locus MLST data. Phylogenetic trees were annotated in iTOL [41].

Generation of closed genomes

For the generation of closed genome sequences, DNA of the bacterial strains was extracted with the GenEluteTM Bacterial Genomic DNA Kit (Sigma). The libraries were prepared with the Rapid barcoding kit (SQK-RBK004, Oxford Nanopore Technologies, Oxford, UK) and afterwards subjected to sequencing in a FLOMIN 106D flow-cell on a MinION device (Oxford Nanopore Technologies, Oxford, UK). The obtained long reads were filtered using the Filtlong tool [42] with standard settings and the following modifications: the minimal length of reads was set to 3000 bp and the target bases to 290,000,000 bp (100-fold coverage). For filtering, the corresponding Illumina reads were used as an external reference. The improved subset of long reads and the Illumina reads were used in a hybrid assembly with Unicycler [43] to generate a closed genome sequence. Genomes were annotated using the NCBI prokaryotic genome annotation pipeline.

Determination of SNP distances

The batchMap pipeline described earlier [20] was used for mapping of sequencing reads against closed reference genomes (Table S2) [44]. This pipeline included (i) read trimming of raw sequencing reads using Trimmomatic, (ii) alignment of trimmed reads to the reference sequence using BWA-MEM, (iii) SAM file-to-BAM file conversion using SAMtools, (iv) pileup using SAMtools mpileup, (v) variant calling using VarScan and (vi) consensus sequence creation. Single nucleotide polymorphisms (SNP) were filtered using the SNPfilter pipeline reported by Becker et al. [45] and an exclusion distance of 300 nt.

Allele calling for virulome and resistome analysis

Known *L. monocytogenes* virulence and resistance genes were included as target loci in a SeqSphere task template [18]. Assembled genomes were queried against these task templates in SeqSphere for the presence or absence of these genes using an identity cut-off of 90% and an alignment coverage cut-off of 99%.

Identification of premature stop codons

We compared the cgMLST and accessory genome MLST (agMLST) allele annotations of the 1802 isolates with a previously generated list of *L. monocytogenes* cg/agMLST alleles affected by internal stop codons [36]. As the cg/agMLST algorithm annotates frameshifted alleles as "failed" alleles, we also inspected the cg/agMLST alleles for the occurrence of failed alleles that are associated with particular sequence types or even specific cgMLST clusters. We considered a gene as inactivated, when an allele variation generated a stop codon between the first 5% and the last 80% of an open reading frame sequence and further included only those genes in the analysis that were affected at least twice within the same phylogroup to exclude accidental sequencing errors.

Identification of hyper- and hypovirulent lineages

For the identification of lineages with differences in virulence potential, we followed the rationale that their differential abilities in host cell invasion, intracellular replication and cell-to-cell spread collectively cumulate in different probabilities of secondary transmission from the liver to the placenta of pregnant women or the central nervous system [26, 46]. Therefore, the number of confirmed cases of materno-foetal infections (MFL) and neurolisteriosis (NL) was counted for the different STs and relative risks for MFL and NL for each ST (ingroup) compared to all other STs as a combined outgroup were

determined. Based on this, risk differences and 95% confidence intervals were calculated according to standard procedures in order to quantify differences in disease outcome and thus virulence potential for the different lineages [47]. STs with significantly increased risks for both types of disease manifestation, MFL and NL, were categorised as hypervirulent, while STs with significantly decreased risks for MFL and NL were considered hypovirulent.

Construction of a Δ*flaR* mutant

To remove *flaR* (*lmo1412*) from the chromosome, regions up- and downstream of *flaR* were amplified using the oligonucleotides SW200 (GATCTATCGATGCATGCC ATGGCGATTAGTTCTGTTATAATGGTTATTAGC)/ SW202 (GCTATTTATCACATTTTAAGCACTCCT TATCTGACTATG) and SW203 (GCTTAAAATGTG ATAAATAGCCCATGAATGCTTGG)/SW214 (GCG CGCGTCGACCAAGTACCATCAAATCAATCCGGA AC), respectively, as primers and fused together by splicing by overlapping extension PCR. The resulting Δ*flaR* fragment was inserted into pHoss1 [48] using NcoI/SalI, and the obtained plasmid (pSW102) was transferred to *L. monocytogenes* EGD-e by electroporation. The *flaR* gene was then deleted following the plasmid insertion/excision protocol of Abdelhamed et al. [48]. Removal of *flaR* and loss of pSW102 was confirmed by PCR and the resulting strain was named LMSW211.

Infection experiments

Infection of J774A.1 mouse macrophages (ATCC® TIB-67™) and HepG2 human hepatocytes (ATCC® HB-8065™) with *L. monocytogenes* strains was performed as described earlier [49]. Briefly, 10^5 cells were seeded into the wells of a 24 multi-well plate and cultivated in DMEM + 10% foetal calf serum (FCS) overnight before they were infected with an inoculum containing 2×10^5 bacteria. The bacteria were allowed to invade the cells and extracellular bacteria were first washed off and the remaining extracellular bacteria were killed by gentamicin. Infected cells were lysed 6 h post infection using ice-cold PBS containing 0.1% Triton X-100; serial dilutions were plated on BHI agar plates and incubated overnight at 37 °C for quantification. Analysis of cell-to-cell spread using 3T3-L1 mouse embryo fibroblasts (ATCC® CL-173T^M) by plaque formation was also carried out as described earlier [50]. Shortly, 5×10^5 fibroblast cells were seeded into the wells of a six well plate and cultivated in DMEM + 10% FCS. After 3 days of incubation, cells were infected with an inoculum of 2, 4 or 10 µl each containing 1×10^6 bacteria. Plaques were stained 3 days post infection using neutral red.

Phenotypic assays

For determination of lysozyme sensitivity, *L. monocytogenes* strains were grown overnight in BHI broth at 37 °C and aliquots of a tenfold dilution series were spotted on BHI agar plates ± 100 µg/ml lysozyme. Agar plates were incubated overnight at 37 °C and then photographed.

For analysis of flagellar motility, strains grown on BHI agar plates were stab-inoculated into LB agar plates containing 0.3% (w/v) agarose. The plates were incubated overnight at 30 °C and photographed the next morning.

In order to visualise wall teichoic acid decoration with N-acetylglucosamine, *L. monocytogenes* cells taken from overnight cultures were diluted 1:100 in fresh BHI and grown for 4 h at 37 °C. Cells from 100 µl aliquots were collected by centrifugation and washed twice with PBS buffer. The washed cells were stained with 0.1 mg/ml CF®488A wheat germ agglutinin conjugate (Biotium, Fremont, CA, USA) in PBS for 5 min at room temperature (22 °C) and washed two more times with PBS buffer. A 0.5 µl aliquot of the stained cell suspension was spotted onto a microscope slide covered with a thin film of 1.5% agarose and covered with a cover slip. Images were taken using a Nikon Eclipse Ti microscope coupled to a Nikon Mono DS-Qi2 CMOS camera and processed using the NIS elements AR software package (Nikon).

Statistics

Levels of significance were determined using a standard two-tailed *t*-test and weighted using the Bonferroni-Holm correction. Values below the threshold of $P < 0.05$ were considered as statistically significant.

Results

Bipartite population structure of clinical *L. monocytogenes* isolates from Germany

In Germany, the detection of *L. monocytogenes* in primary sterile clinical specimens and in swabs from newborns has to be notified to public health authorities, while the bacterial isolates can be sent to the Consultant Laboratory (CL) for *Listeria* at the Robert Koch Institute for further analysis on a voluntary basis. Between 2018 and 2021, 2464 cases of human listeriosis were notified in Germany and 1802 clinical *L. monocytogenes* isolates were received by the CL. 1538 of the 1802 isolates (85%) were allocated to a notified case, while 264 isolates (15%) were sent to the CL but specific allocation to a notified case was not possible. Thus, *L. monocytogenes* isolates were available and assignable for 62% of the notified listeriosis cases in Germany. The portion of notification cases with accompanying isolate submissions ranged from 26 to 74% depending on the federal country (Fig. 1).

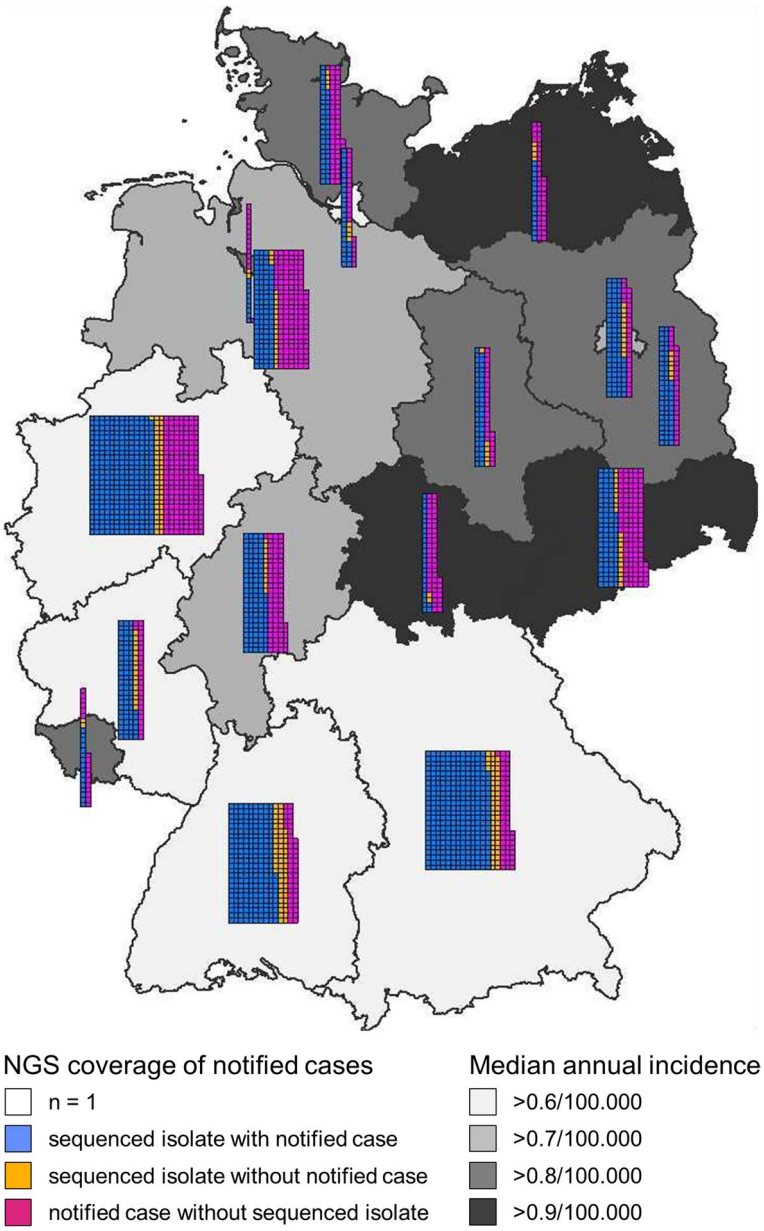

Fig. 1 WGS coverage of human listeriosis cases in Germany, 2018–2021. Geographic origin of 2464 notified listeriosis cases and 1802 isolate submissions in Germany during 2018–2021. The numbers of notified cases that were accompanied by isolate submissions, the numbers of notified cases without isolate submissions and of isolate submissions for which no notification was initiated are shown for each of the 16 German federal countries. The median incidence per year for the 2018–2021 period is also shown for each federal country

The genomes of all *L. monocytogenes* strains were sequenced and molecular serogroups were extracted from sequencing data. The majority of the isolates belonged to molecular serogroups IVb ($n=830$; 46%), IIa ($n=781$; 43%) and IIb ($n=164$; 9%), whereas only few isolates were of serogroup IIc ($n=14$), IVbv-1 ($n=10$), IVa ($n=2$) and IVc ($n=1$) (Fig. 2). Thus, the population primarily is made up of isolates belonging to phylogenetic lineages I and II (Fig. 2), while isolates belonging to other lineages are not found or were underrepresented. Multi-locus sequence typing (MLST) showed that sequence types (ST) ST6 ($n=300$; 17%), ST1 ($n=266$; 15%), ST8 ($n=209$; 12%), ST2 ($n=91$; 5%) and ST451 ($n=76$; 4%) were the five most prevalent STs (Fig. 3A). In total, the 1802 isolates grouped into 109 different MLST STs in 59 MLST clonal complexes (CCs) (Fig. 2, Table S1). For 5 STs, a CC number has not been defined yet.

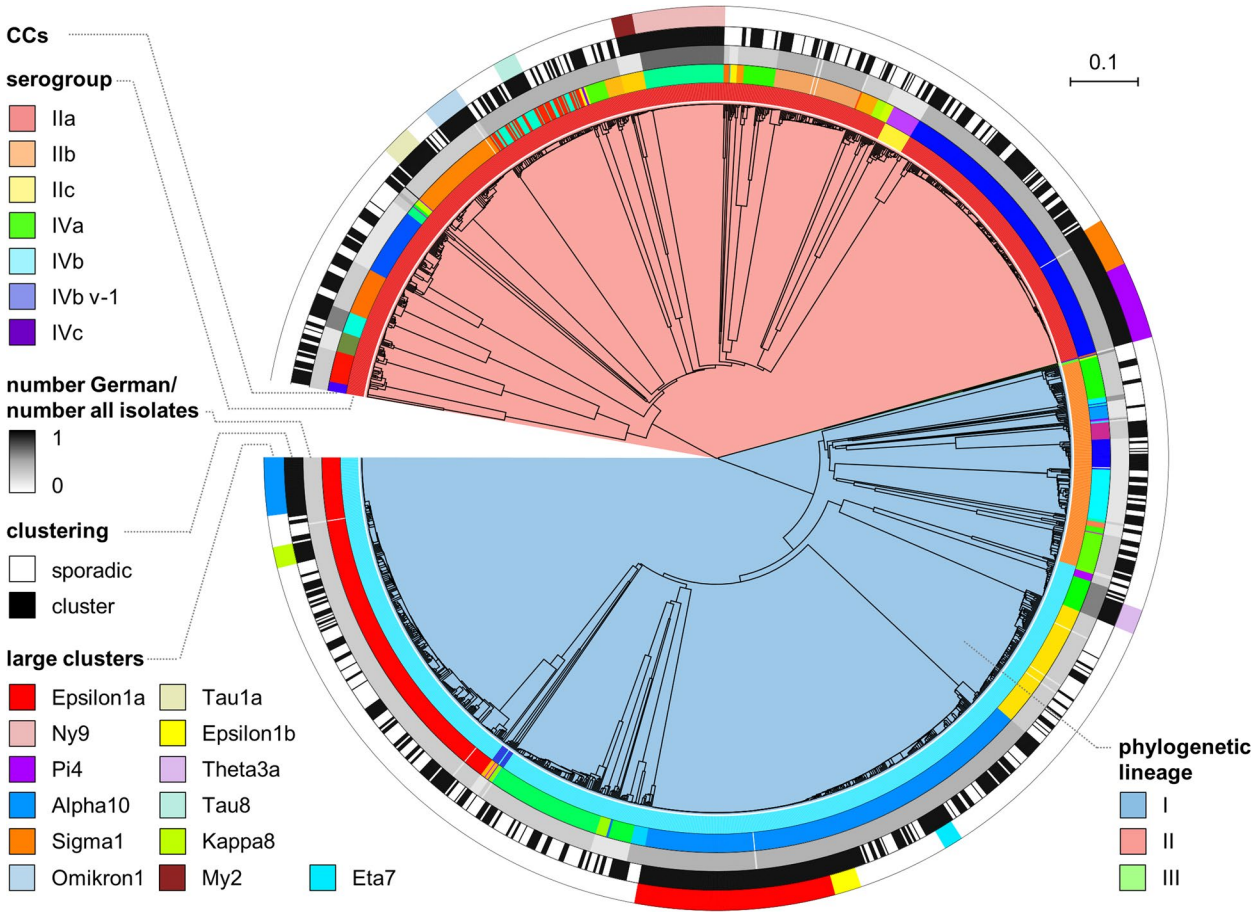

Fig. 2 WGS-based subtyping of clinical *L. monocytogenes* strains from Germany. Unrooted UGPMA tree showing the population structure of 1802 clinical *L. monocytogenes* isolates collected between 2018 and 2021 in Germany. The tree was calculated from 1701 locus cgMLST data. Phylogenetic lineages are indicated by the inner colouring. Outer rings visualise the different molecular serogroups, the different and clonal complexes ("CCs") according to 7 locus MLST, the frequency of German CCs compared to CCs present among 15,156 international NCBI genomes (number German/number all isolates) and the attribution of isolates to an outbreak cluster according to cgMLST as described in the text ("clustering"). The largest outbreaks in this period are highlighted at the outmost circle ("large clusters"). International spread of the CCs observed in Germany is expressed as the number of German isolates divided by the number of all (German + known non-German) isolates for each CC in the grey shaded ring. The scale bar indicates the number of allelic substitutions per locus

Comparison with global clinical *L. monocytogenes* isolates identifies autochthonous STs

We wondered whether there are major genomic differences between clinical *L. monocytogenes* in Germany and isolates collected in other countries. In order to address this, we downloaded the assembled genomes of all clinical *L. monocytogenes* isolates with non-German origin that had been deposited on the NCBI pathogen detection server until 21st September 2022. This included 15,156 genomes from strains isolated between 1921 and 2022 (where reported), with more than 90% of the strains isolated since 2006. The assembled genomes were 2.7–3.6 Mbp in length (median: 3.0 Mbp) and contained 1–489 contigs (median 23). Strains came from 48 different countries from all world regions (Fig. S1A); however, isolate genomes from the USA ($n = 7899$) and the UK ($n = 1568$) were the most frequent (Fig. S1B). A MLST ST could be assigned to 97.3% of the downloaded genomes, resulting in a diversity of 959 different STs.

Comparison of the ST assignments for isolates from inside and outside Germany showed that the majority of STs/CCs observed in Germany (80% of the German STs covering 98.5% of the German isolates) were also reported to cause disease outside Germany (Fig. 2). Likewise, German isolates were found in most of the phylogenetic branches of pathogenic *L. monocytogenes* from locations outside the country (Fig. S1C), suggesting a cross-country distribution of pathogenic *L. monocytogenes* STs in general. However, an overrepresentation of ST249 isolates (CC315) was observed

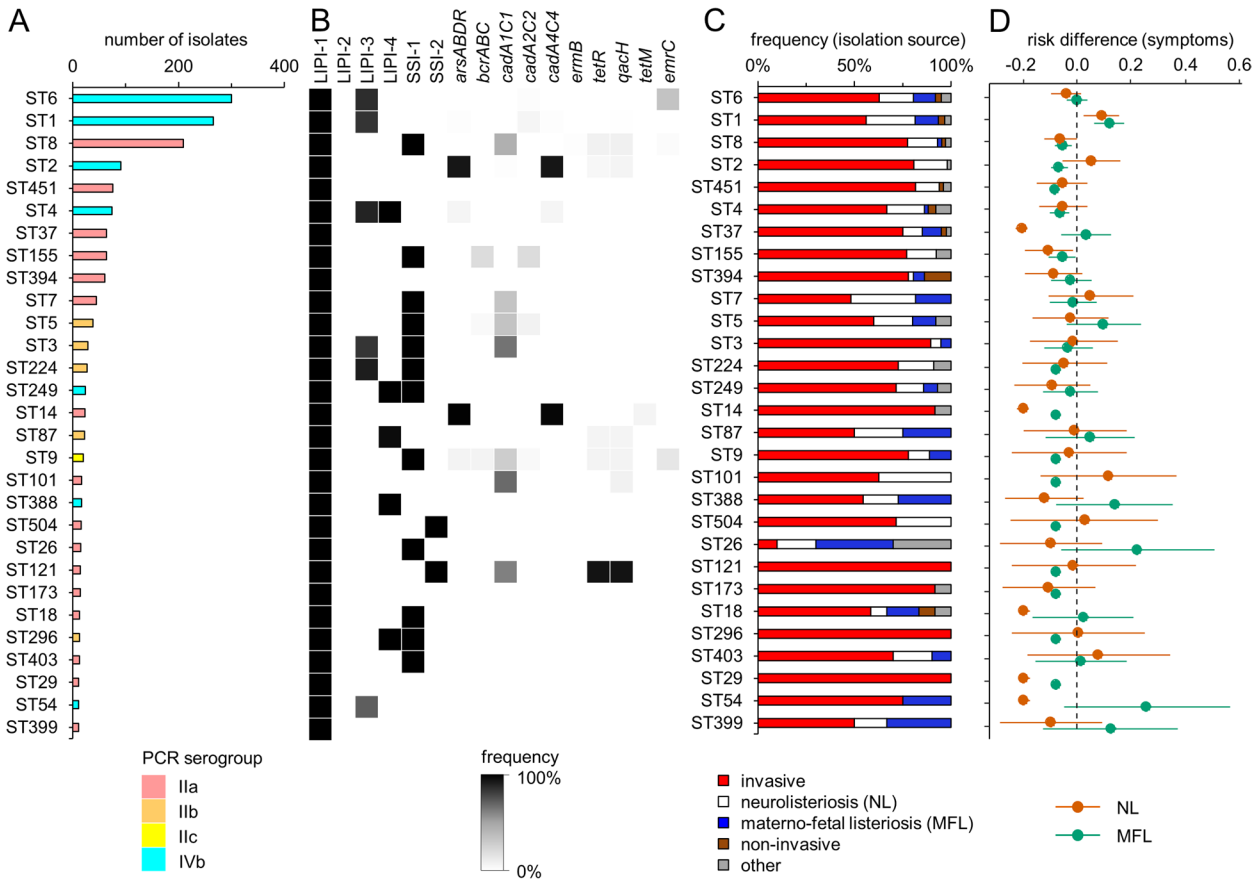

Fig. 3 Genomic and clinical characteristics of the most prevalent *L. monocytogenes* STs. **A** Distribution of sequence types among the collection of German *L. monocytogenes* isolates. Only STs with more than 10 isolates are shown. Bars are coloured according to their molecular serogroup. **B** Presence of the four *L. monocytogenes* pathogenicity islands (LIPI), the two stress survival islets (SSI) and selected resistance genes within the different STs. Grey shading reflects the prevalence of a given marker within all analysed isolates of the respective ST. **C** Clinical disease manifestation as reported during isolate submission to the consultant laboratory. For 1113 out of the 1802 isolates, information on the disease manifestation was available and grouped into five different categories. **D** Clinical disease manifestation as reported during case notification. Risks for NL and MFL manifestations are expressed as risk differences together with 95% confidence intervals. Abbreviations: NL neurolisteriosis, MFL materno-foetal listeriosis

among the clinical 2018–2021 strains from Germany compared to the international sequences, as 24 clinical ST249 isolates have been collected in Germany and only one is known from outside Germany (Slovenia). Likewise, 14 clinical ST173 isolates from Germany, but only 7 from locations outside Germany, in particular from the Netherlands and the UK were detected. While the German and the Slovenian ST249 isolates are not closely related, all ST173 isolates belong to the same cgMLST cluster (My2, Table S1), reflecting a cross-country outbreak [25]. Thus, ST249 and ST173 show limited geographic distribution and therefore may represent autochthonous clones in Germany. In contrast, 868 STs, which are associated with disease outside Germany, are not present in the German 2018–2021 collection. Of these, ST321, ST378 and ST389, predominantly from the USA, New Zealand and/or Taiwan, had the largest number of non-German isolate genomes available at the NCBI server at the time of analysis.

Virulome and resistome differences among frequent clinical subtypes

Allele calling showed that *Listeria* pathogenicity island 1 (LIPI-1) was present in the genomes of all German isolates, while LIPI-2, typically present in *L. ivanovii* [51] or as a truncated version in the novel hybrid sublineage HSL-II [52], was not found in any of them (Fig. 3B). For the STs with > 10 isolates, LIPI-3, encoding listeriolysin S [53], was detected in ST1, ST3, ST4, ST6 and ST224 isolates as well as in approximately half of the ST54 isolates, corresponding to 35% of all isolates. LIPI-4 associated with neuro-invasion [26] was found in ST4, ST87, ST249, ST296 and ST388 isolates (11% of all isolates). Thus, ST4 was the only group among the more frequent STs that

contained three of the four known pathogenicity islands (Fig. 3B), while LIPI-3 and LIPI-4 were generally absent from lineage II and III isolates.

Stress survival islet SSI-1 supporting growth at low pH and high salt conditions [54] was found in 31% of the isolates belonging to different STs, while SSI-2 promoting growth under alkaline and oxidative stress [27] was present only in ST121 and ST504 strains (2% of all isolates). We also observed that 92% of the ST2 and > 98% of the ST14 strains contained the *arsABDR* and *cadA4/cadC4* resistance genes encoding heavy metal resistance determinants [55, 56] and that 93% of the ST121 strains carried the *qacH* and *tetR* genes for tolerance against quaternary ammonium compounds [57] (Fig. 3B).

The presence of acquired antibiotic resistance genes (*aad6*, *cat*, *ermB*, *tetM*, *tetS* and *dfrG*) was also tested, but only two *tetM* (two sporadic isolates) and two *ermB* positive isolates (CT9067) were found.

Analysis of clinical metadata highlights st1 isolates as hypervirulent

Information on the disease manifestation and/or isolation source accompanied isolate submissions for 1113 of the 1802 isolates (62%). Out of these, 69% of the isolates were from invasive listeriosis cases (isolation from blood, ascites, synovial, pleural or lymph fluid, abscesses, wounds and histologic specimens or from patients suffering from sepsis, bacteraemia or fever), 17% from invasive neurolisteriosis (NL) patients (isolation from cerebrospinal fluid or from patients with meningitis or encephalitis), 7% from materno-foetal listeriosis (MFL), 2% from non-invasive conditions (stool) and 5% from other manifestations. Remarkably, there were no ST14, ST29, ST121, ST173 and ST296 isolates from MFL or NL samples according to this set of data (Fig. 3C). To identify phylogenetic lineages with differences in virulence potential, we determined the risk differences for MFL or NL associated with infections caused by different *L. monocytogenes* STs using notification data. This data is based upon reported details from the local health authorities on disease manifestation and/or symptoms. Information on the establishment of MFL ($n = 98$ cases), NL ($n = 203$) or not was available for 1323 isolate/notification case pairs in total. Relative risks for MFL and NL were both reduced for infections caused by ST8, ST14, ST29 and ST155 strains (all belonging to serogroup IIa) but increased for infections caused by ST1 strains (serogroup IVb, Fig. 3D). Thus, these STs were here referred to as hypo- and hypervirulent, respectively. We further noticed that several STs were associated with reduced risks to establish MFL (ST2, ST4, ST9, ST101, ST121, ST173, ST224, ST296, ST451, ST504) or NL only (ST18, ST37, ST54) (Fig. 3D). ST1 patients were significantly younger than all other listeriosis patients ($P = 3.5 \times 10^{-5}$, *t*-test with Bonferroni-Holm correction). The higher number of MFL cases (that are of younger age) among the ST1 infections explains this effect, since no differences were observed when MFL cases were excluded. Differences in age distribution were not found for any of the other STs. At the serogroup level, infections with serogroup IIa strains were associated with reduced MFL and NL risks, while an above average MFL risk was detected for IVb infections (Fig. S2), to which hypervirulent ST1 belongs (Fig. 3D).

Information of patient sex was available for 1550 isolates (86% of all isolates), according to which 42% were isolated from female patients ($n = 652$) and 58% were from men ($n = 898$). When MFL were excluded, general differences in sex distribution among patients infected with the 29 most prevalent STs shown in Fig. 3A were not detected, but a significant overrepresentation of female patients among all ST37 infections was observed (61% female, 39% male, $P < 0.05$, χ^2-test).

In vitro strain virulence corresponds to risk potential of hyper- and hypovirulent sts

We selected one representative isolate per hyper- and hypovirulent ST identified above to test them in cell culture infection experiments. Strain selection was made based on cluster size (Table 1) and/or the availability of closed genome sequences. This selection included strain 18-04540 from the large Epsilon1a outbreak [18] as a representative for ST6 with average MFL/NL risk (Fig. 3D), strain 21-03201 from the Alpha10 cluster representing hypervirulent ST1, strain 19-05816 from the Pi4 cluster [44] for hypovirulent ST8, strain 19-06323 (Chi1a cluster) as a hypovirulent ST14 isolate, the sporadic 21-04322 strain representing hypovirulent ST29 and the Omikron1 strain 17-01049 as a member of hypovirulent ST155.

First, intracellular multiplication of these strains was determined in J774 mouse macrophages, but differences in uptake or intracellular replication were not observed (data not shown). Likewise, all strains formed plaques in 3T3 mouse fibroblasts indicating normal cell-to-cell spread (not shown). However, when the same experiment was repeated with HepG2 human liver cells, differences became apparent: For hypervirulent ST1, we generally observed a slightly increased invasion into HepG2 cells (compared to the reference ST6 isolate) in all experiments (1.5 ± 0.3 fold in the experiment shown in Fig. 4). This was consistently found in all experiments but only reached statistical significance in 3 out of 4 repetitions. In contrast, invasion efficiency of hypovirulent ST8 ($12 \pm 4\%$ of the ST6 invasion level), ST14 ($0.8 \pm 0.5\%$) and

Table 1 Key characteristics of German listeriosis clusters with ≥ 10 isolates in 2018–2021

Cluster name	Isolate number	Molecular serogroup	MLST ST	Clonal complex	cgMLST CT	Source of infection	Cases abroad[a]	Reference
Epsilon1a	132	IVb	ST6	CC6	CT4465, CT7353	Blood sausage	Yes	[18]
Ny9	61	IIa	ST394	CC415	CT13516, CT14488	Rainbow trout	Yes	[58]
Pi4	51	IIa	ST8	CC8	CT5004	Unknown	Unknown	This work
Alpha10	38	IVb	ST1	CC1	CT6329	Unknown	Unknown	This work
Sigma1	32	IIa	ST8	CC8	CT2521	Meat products	Unknown	[31]
Omikron1	25	IIa	ST155	CC155	CT1128	Salmon products	Yes	[25]
Tau1a	20	IIa	ST155/ST2890	CC155	CT2198	Salmon products	Yes	[25]
Epsilon1b	18	IVb	ST6	CC6	CT90, CT4465	Unknown	Unknown	This work
Theta3a	17	IVb	ST249	CC315	CT4449, CT6762, CT8445, CT13943	Unknown	Unknown	This work
Tau8	16	IIa	ST451	CC451	CT9031	Unknown	Yes	This work
Kappa8	14	IVb	ST1	CC1	CT4961, CT14526	Unknown	Yes	This work
My2	14	IIa	ST173	CC19	CT3242	Salmon products	Yes	[25]
Eta7	13	IVb	ST6	CC6	CT7504	Unknown	Yes	This work
Psi1	13	IVb	ST1	CC1	CT4246	Unknown	Unknown	This work
Omega5	12	IIb	ST87	CC87	CT773, CT1138	Salmon products	Yes	[25]
Sigma5	12	IIa	ST504	CC475	CT5715	Salmon products	Unknown	[25]
Gamma5a	11	IIb	ST296	CC88	CT1703, CC6766	Unknown	Unknown	This work
Gamma6a	11	IIa	ST8	CC8	CT4172	Unknown	Unknown	This work
Beta2a	10	IIa	ST8	CC8	CT1247	Salmon products	Yes	[25]
Ypsilon1a	10	IVb	ST1	CC1	CT2752	Unknown	Unknown	This work
Zeta5a	10	IVb	ST6	CC6	CT3386	Salmon products	Yes	[25]

[a] According to requests to all EU member states via the EPIS platform after outbreak detection

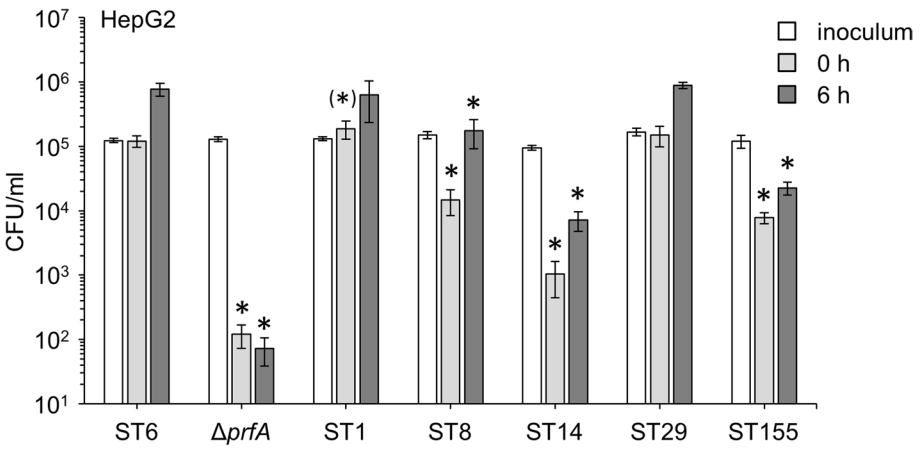

Fig. 4 In vitro virulence of hyper- and hypovirulent STs. Invasion of and intracellular replication in HepG2 hepatocytes by representative *L. monocytogenes* strains belonging to hyper- and hypovirulent STs identified in this study. Strains tested were 18-04540 (ST6, Epsilon1a), 21-03201 (ST1, Alpha10), 19-05816 (ST8, Pi4), 19-06323 (ST14, Chi1a), 21-04322 (ST29, sporadic isolate) and 17-01049 (ST155, Omikron1). The experiment was carried out as triplicate and average values and standard deviations were calculated. Asterisks mark statistically significant differences compared to ST6 (*t*-test with Bonferroni-Holm correction, $P < 0.05$)

ST155 strains (6 ± 0.3%) was significantly reduced. Consequently, final bacterial loads 6 h post infection were also reduced to 22 ± 10% (ST8), 0.9 ± 0.2% (ST14) and 2.9 ± 0.6% of the ST6 reference level in the hypovirulent STs. In contrast, the ST29 isolate did not reveal an invasion or replication defect (Fig. 4) as suggested by its

reduced disease severity (Fig. 3D). This shows that the ability to invade hepatocytes corresponds to the risk potential of the different STs to establish MFL and NL and is therefore of key importance for disease severity.

Size, duration and geographic distribution of listeriosis clusters

For determination of disease clusters, the 1802 genomes were consecutively analysed by cgMLST using an initial threshold of ≤ 10 allele differences for cluster definition. For communication of a large number of outbreaks within the public/veterinary health offices, cgMLST clusters were named in the sequence of their detection using a nomenclature combining a Greek letter with a continuous number (i.e. Alpha1, Beta1,…Omega1, Alpha2, Beta2 and so on) that we had established for the German listeriosis surveillance system. Since March 2020, the cgMLST cluster cut-off was set to ≤ 7 allele differences, since larger distances were not observed in epidemiologically confirmed outbreaks [18, 30–32, 49]. Clusters that could be differentiated into subclusters using the new threshold were labelled by additional letters (e. g. Epsilon1a, Epsilon1b,…). Over the 4 years, this approach grouped 1129 of the 1802 isolates (63%) into a cgMLST cluster and classified 673 isolates (37%) as sporadic (Fig. 2), which differed in > 7 cgMLST alleles from their next relatives [59]. As a result, isolates belonging to 253 different cgMLST clusters are included in the 2018–2021 isolate collection. For 65 of these clusters, only one isolate fell into the study period; the remaining 188 clusters included 2–132 isolates (median: 3). The five largest clusters were Epsilon1a (132 isolates) [18], Ny9 (61 isolates) [58], Pi4 (51 isolates), Alpha10 (38 isolates) and Sigma1 (32 isolates) [31] (Fig. 2, Table 1).

We defined cgMLST clusters as acute when all isolates belonging to this cluster were collected within 12 months and all remaining clusters as protracted. This grouped the 188 cgMLST clusters, into 109 acute and 79 protracted clusters (Fig. S3A). The average period of activity of all these clusters together was 1.1 years (median: 0.7 years).

To determine their geographic distribution, we counted the number of federal countries for each cluster. Out of the 188 clusters, 75 clusters (40%) had cases in only one of the 16 German federal states and included 2–13 isolates (median: 2); we consider them as regional clusters. The remaining 113 clusters (60%) were considered cross-regional clusters, affected 2–13 federal states (median: 3) and included a higher number of isolates: 2–132 (median 4, Fig. S3B). Clinical isolates matching several of these clusters from other European countries were identified through requests through the Epidemiological Intelligence System (EPIS) platform of the European Centre for Disease Control (ECDC), indicating that several outbreaks even generated cases on the European scale (Table 1).

Important german listeriosis clusters in 2018–2021

Twenty-one cgMLST clusters included ≥ 10 isolates out of which several clusters (Epsilon1a, Ny9, Sigma1) had been traced back to their infection sources and stopped [18, 31, 58] (Table 1). Seven more clusters with ≥ 10 isolates were linked to salmon consumption [25] (Table 1). However, several other large clusters (Pi4, Alpha10, Epsilon1b, Theta3a, Kappa8, Eta7) could not be traced back to their source yet (Table 1).

Pi4 comprised 51 isolates between 2018 and 2021 forming a contiguous cluster that differed in 0–16 cgMLST alleles from each other (Fig. 5A). Pi4 is geographically widespread in Germany, protracted (Fig. 5B–C) and closely related to but distinct from the clone, which caused the German Sigma1 outbreak recently (12–23 different cgMLST alleles) [31].

Alpha10 consists of 38 isolates (Table 1) and is highly clonal (0–3 alleles difference). Reconstruction of the closed genome of a representative Alpha10 isolate (21-03201, Table S2) and SNP calling showed that the Alpha10 isolates differed in 0–3 SNPs only. The majority of the Alpha10 isolates was collected in 2021 in South-Western Germany (Fig. 5B–C).

Epsilon1b includes 18 isolates (Table 1). In agreement with its protracted character (Fig. 5B), Epsilon1b is more heterogeneous and its isolates are distinguished from each other by 0–17 cgMLST alleles and 0–21 SNPs, with the reconstructed genome of Epsilon1b strain 11–04869 (Table S2) used as the reference. The Epsilon1b clone can be differentiated from the Epsilon1a clone, which caused the largest outbreak of invasive listeriosis detected in Germany so far [18], by the presence of a 42 kb prophage at the $tRNA^{Lys}$ locus, which was collectively absent from the Epsilon1a isolates (Fig. S4).

Theta3a represents another protracted cluster and contains 17 isolates (Fig. 5B). Theta3a isolates belong to ST249, which are overrepresented in Germany (see above) and were collected from the North-Eastern and Western federal countries. They differ in 0–19 cgMLST alleles from each other and by 2–25 SNPs after variant calling using a reconstructed Theta3a genome (16–02236, Table S2) as the reference. Theta3a (ST249) constitutes a deeply branching clade within serogroup IVb. Interestingly, all ST249 strains carried an internal stop codon in *ispG* (ORY89_07620, *lmo1441* in EGD-e) (Table S3).

The Kappa8 cluster reflects a rather acute epidemiological incident with 14 isolates from Southern and Eastern Germany (Fig. 5B–C) that differed in 0–7 cgMLST alleles (median: 2) and 0–7 SNPs (median: 2) with the

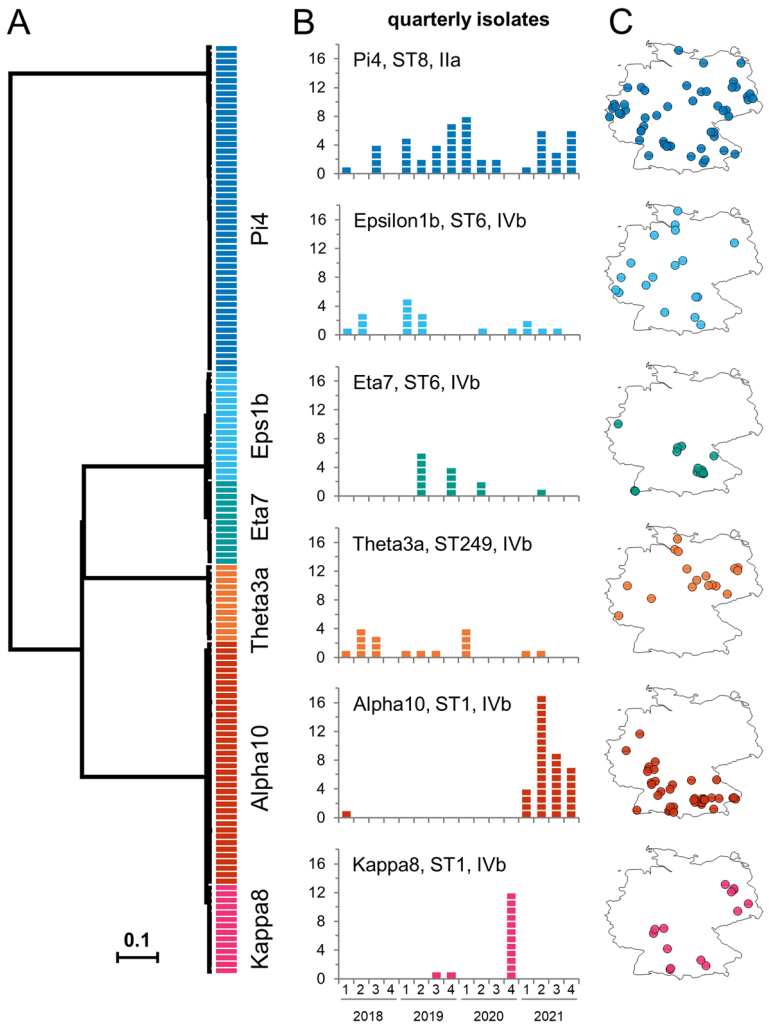

Fig. 5 Large German listeriosis clusters with unknown infection source. **A** Unrooted UPGMA tree calculated from 1701 locus cgMLST data for the German listeriosis clusters Alpha10, Epsilon1b, Eta7, Kappa8, Pi4 and Theta3a. Isolates collected in 2018–2021 were included. The scale bar indicates the number of allelic substitutions per locus. **B** Epidemiological curves for the same clusters based on isolate collection dates. **C** Geographical origin of isolates within Germany

reconstructed genome of Kappa8 strain 19–07394 (Table S2) as the reference.

Eta7 is a cluster with pathogen isolation in West and South Germany (Fig. 5B). The 13 Eta7 isolates differed in 0–5 (median: 2) cgMLST alleles and 0–9 SNPs (median: 7) using the genome of Eta7 strain 19–02390 as the reference (Table S2). Remarkably, 12 of the 13 Eta7 isolates were collected from newborns or pregnant women.

Maintenance of virulence and fitness gene function in hypervirulent ivb isolates

To explain reduced MFL and NL risks of hypovirulent STs, we inspected the LIPI-1 and *inl* internalin genes for the presence of premature stop codons (PMSCs) and frameshifts. Inactivating mutations were not found in the LIPI-1 and *inlB*, *inlC*, *inlE*, *inlGH*, *inlI*, *inlJ*, *inlL* and *inlP* genes in any of the clinical isolates, but were present in *inlA* of all ST121 isolates and in several ST9 clones (Table S3). Moreover, all Tau8 strains (ST451) carried a PMSC in the *inlF* gene (Table S3). InlF was reported to support the uptake of *L. monocytogenes* by mouse macrophages [60]. However, the *inlF*$^-$ Tau8 isolate 20-01331 was taken up and replicated to the same bacterial titre in J774 mouse macrophages as efficiently as the EGD-e wild type or two other InlF positive ST451 strains belonging to the Xi5 and Omikron5 clusters (Fig. 6A).

Comparison of cgMLST/agMLST allele numbers with a previously generated list of inactivated *L. monocytogenes* alleles [36] further detected inactivating mutations in the autolysin encoding *aut* gene in several clones belonging

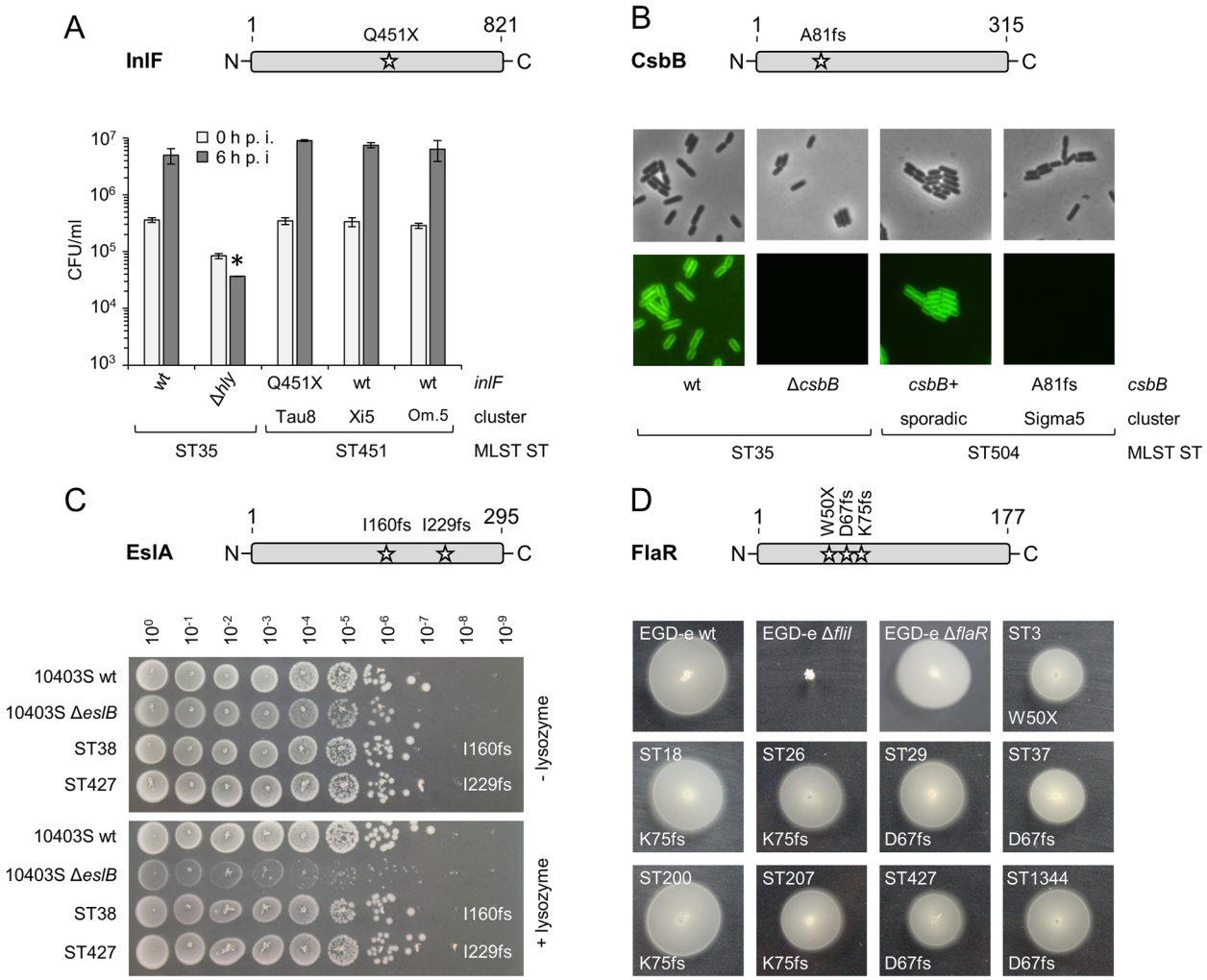

Fig. 6 Phenotypes of clinical isolates with inactivated *inlF*, *csbB*, *eslA* and *flaR* genes. **A** A premature stop codon inactivates the *inlF* gene of Tau8 isolates (ST451, CT9031). Scheme showing the position of the Q451X mutation within *inlF* of Tau8 strains (upper panel). Despite inactivated *inlF*, the Tau8 isolate 20-01331 shows full virulence in a mouse macrophage infection assay (lower panel). J774 mouse macrophage were infected with *L. monocytogenes* strains EGD-e (ST35, wt), LMS250 (ST35, Δ*hly*), 20-01331 (Tau8, ST451, InlF truncated), 18-03445 (Xi5, ST451, full-length InlF) and 18-02122 (Omikron5, ST451, full-length InlF) and the bacterial titre was determined right after infection (0 h p. i.) and 6 h later (6 h p. i.). Average values and standard deviations were calculated from technical triplicates. The asterisk indicates a statistically significant difference ($P < 0.01$, *t*-test with Bonferroni-Holm correction). Abbr.: Om.5 Omikron5. **B** Sigma5 isolates (ST504, CT5715) carry an inactivated *csbB* gene. Scheme illustrating the position of the A81fs mutation within *csbB* of Sigma5 strains (upper panel). Micrographs of *L. monocytogenes* strains 20-06257 (ST504, CT14635, sporadic, *csbB*$^+$) and 21-06873 (ST504, CT5715, Sigma5, *csbB* A81fs) after staining with fluorescently labelled wheat germ agglutinin (lower panel). Phase contrast (top row) and fluorescence images (bottom row) are shown. ST35 strains EGD-e (wt) and LMJR156 (Δ*csbB*) were included as controls. **C** ST38 and ST427 isolates carry *eslA* inactivating mutations. Scheme showing the position of the inactivating mutations within *eslA* (upper panel). Spot dilution assay to determine lysozyme resistance of representative ST38 (20-02710) and ST427 (21-00930) isolates on BHI agar plates ± lysozyme (lower panel). ST87 strains 10403S (wt) and ANG4275 (10403S Δ*eslB*) mutant were included as controls. **D** Mutations inactivating the *flaR* gene in various subtypes. Scheme showing the position of *flaR* inactivating mutations (upper panel). Swarming assay to test flagellar motility of representative ST3 (18-04580), ST18 (18-00242), ST26 (19-02197), ST29 (18-03980), ST37 (20-01921), ST200 (18-02068), ST207 (20-01871), ST427 (18-01591) and ST1344 (21-01230) isolates (lower panel). Isogenic strains EGD-e, LMSW211 (Δ*flaR*) and LMS3 (Δ*fliI*, all belonging to ST35) were included as controls. Respective STs and their *flaR* mutations are indicated

to the ST3, ST121 and hypovirulent ST155 sublineages and an inactivating mutation in the *chiB* chitinase gene in several ST4 isolates (Table S3). PMSCs were also identified in the chitin binding protein encoding *lmo2467* gene in the majority of the hypovirulent ST29 isolates and in the My5 cluster belonging to ST9 (Table S3).

The *csbB* gene, required for decoration of wall teichoic acids with N-acetylglucosamine (GlcNAc) [61], carried

frameshift mutations in clones belonging to ST87 and ST504. Fluorescent lectin staining to detect the presence of GlcNAc-modified wall teichoic acids (WTA) showed that WTAs of the *csbB*$^-$ Sigma5 (ST504) isolate 21-06873 were indeed not decorated with GlcNAc as expected, whereas no such defect was observed in a related sporadic *csbB*$^+$ ST504 isolate (Fig. 6B). We also found that the *eslA* gene, encoding the ATPase of the EslABC transporter, which contributes to lysozyme resistance [38], was frameshifted in all ST38 and ST427 isolates (Table S3). However, two selected ST38 and ST247 strains showed the same resistance to lysozyme as wild type strain 10403S in contrast to its isogenic Δ*eslB* mutant (Fig. 6C).

The *clpP1* protease gene of all nine ST16 strains and the *ispG* gene from the non-mevalonate pathway of all ST249 strains were also truncated. ST16 belongs to the same clonal complex as hypovirulent ST8, while ST249 is a sublineage within serogroup IVb, but one with an average disease severity scores (Fig. 3D). The motility gene *flaR* was truncated in most ST3 isolates and frameshifted in most if not all ST18, ST26, hypovirulent ST29, ST37, ST200, ST207, ST427 and ST1344 strains (Table S3). However, motility of representative isolates from these *flaR*$^-$ STs and of a Δ*flaR* deletion mutant was not impaired (Fig. 6D).

Remarkably, 23% of the IIa (hypovirulent), half of the IIc (reduced MFL risk) and 20% of the IIb isolates (average MFL/NL risk) carried one of the mutations identified above, but only 4% of the IVb isolates (hypervirulent), and out of these only ST249 (*ispG*) as well as some ST4 isolates (*chiB*) were affected (Table S3). Thus, it seems that purifying selection maintains the function of these genes in the majority of the IVb isolates. Moreover, the importance of these genes for *L. monocytogenes* biology originally established in reference strains cannot be generalised.

Discussion

Population structure and disease clusters

The combination of sequencing data covering the majority of clinical cases with notification data enabled us to analyse human *L. monocytogenes* infections that occurred in Germany over a period of four consecutive years in different dimensions. First, we observed the same bipartite population structure as described by others [62, 63] with two genetically distinct lineages that each contributed to almost equal parts to listeriosis cases in Germany: phylogenetic lineage I (comprising serogroups IIb, IVb, IVbv-1) and phylogenetic lineage II (IIa and IIc), whereas strains of other lineages were only found rarely or not at all. Separation into two well-separated lineages likely reflects pathogen adaptation to different environmental or animal reservoirs. Second, the overall population structure did not change much compared to a previous analysis covering isolates from 2007 to 2017 [20]. During both periods, serogroups IVb, IIa and IIb as well as sequence types ST6, ST1 and ST8 were the three most prevalent phylogenetic groups in Germany [20]. Despite their high isolation frequency, ST6, ST1 and ST8 isolates are not characterised by a higher number of pathogenicity islands, stress or resistance genes, suggesting that other factors explain their predominance. Clonal expansion in the past or stable colonisation of environmental habitats and infection sources with established and persistent clones, respectively, and rarely occurring infiltration of these niches by new subtypes from external ecosystems could explain this observation [64]. Furthermore, the majority of isolates belonged to cgMLST clusters, out of which more than the half of the clusters generated cases on a cross-regional scale. Thus, foodstuff produced for supra-regional retail rather than local production and consumption accounts for most listeriosis cases in Germany. A significant portion of the listeriosis clusters also is active for more than 12 months, which would be consistent with (i) constant pathogen dissemination from environmental sources into the food processing chain, (ii) persistent contamination of food processing facilities with the same clone or (iii) long-term storage of contaminated products in patient households. At least for the latter two scenarios, several published examples exist that made them appear plausible [30, 65, 66]. Several of the clusters identified also reflected known listeriosis outbreaks (Table 1). Their recognition can initiate successful back-tracing of *L. monocytogenes* clones to their infection source as demonstrated during past outbreaks [17–19].

Risk profiling of prevalent clinical *L. monocytogenes* subtypes

Besides its importance for public health, genomic pathogen surveillance also allows the identification of hypo- and hypervirulent subtypes or regionally prevailing clones, when genomic subtyping data are combined with information on disease severity or geographic data, respectively. Using this type of approach, the second most prevalent subtype (ST1) turned out as hypervirulent compared to most prevalent ST6 showing average risk potential for development of MFL/NL, while others (ST8, ST14, ST29 and ST155) generated less MFL and NL cases. Remarkably, ST1 strains had also been associated with increased rates of MFL/NL infections by other authors [26, 46], and classification of ST8 and ST155 strains as less virulent further validates our data, as this is consistent with the reduced rates of MFL/NL infections or their experimentally proven hypovirulence, respectively, reported in other studies [26, 67]. Furthermore,

hypovirulence of ST14 isolates seen here is in accordance with their reduced in vitro invasion efficiency into Caco-2 cells [68] and their previous classification as an environment-associated subtype [69]. However, this view is challenged by reports showing increased virulence in *Galleria* infection assays of CC14 [70]. ST29 represents a newly discovered subtype associated with reduced MFL/NL rates. This is congruent with the detection of ongoing gene loss (*flaR*, *lmo2467*) in this phylogenetic clade (this work), probably resulting in fitness defects at least under certain conditions. The observation that several STs were associated with decreased risks for MFL or NL without affecting the risk for the respective other disease condition is consistent with the idea that pathogen transmission to the brain and the placenta is supported by specific sets of virulence factors, the functionality of which can be impaired independently from each other. However, inactivation of the known determinants for brain (*inlF*) [71] or placenta invasion (*inlP*) [72] did not explain the occurrence of several STs with reduced risk for either MFL or NL. We also did not detect a significantly reduced NL risk associated with Tau8 infections (truncated *inlF*), but the small number of Tau8 patients, for which clinical data were available, has probably hampered detection of a significant effect. Significant associations were found between disease manifestations and serogroups, while presence, absence or total number of pathogenicity islands was not associated with disease forms. Quantification of such associations in our approach is surely masked by non-genetic confounders such as consumer behaviour, possible biases in the differential consumption of outbreak-associated food items in certain risk groups or other patient-associated influences. As further limitations, data on disease manifestation was not available for all isolates/cases and data on the immune status or comorbidities were not generally available. Despite these limitations, our study represents one of the very few surveys currently available [26] that combines genomic pathogen typing data with clinical data on disease outcome from a systematic national sampling program that almost achieves full case coverage. Our analysis also suggests that further genetic factors determining infection of the brain and the placenta may exist, as secondary organ involvement has to be considered a multifactorial process [46].

Further benefits of genomic surveillance systems

As another benefit, genomic pathogen surveillance allows the measurement of the frequency of natural gene loss that occurs in clinical pathogen populations. Since the majority of our isolates were collected from invasive listeriosis, i.e. isolated from primary sterile body fluids, genes found to be inactivated by PMSCs or frameshift mutations in a sufficient number of isolates (e.g. *csbB*, *clpP1*, *eslA*, *flaR*, *inlA* or *inlF*) are likely not essential for pathogen transmission from the gut to the blood stream per se. In this way, genomic pathogen surveillance provides an unbiased possibility to verify or relativise data on the importance of selected genes for *L. monocytogenes* virulence that had been deduced from in vitro or animal studies. For example, even though ClpP1 is secondary to ClpP2, and only supports ClpP2 function [73], we were actually surprised to see that *clpP1* can be lost in clinical isolates having caused invasive disease, since ClpP proteins have crucial roles in protein homeostasis [74]. Apparently, *clpP1* likely is an accessory or even remnant gene that is not essential for survival in the environment or during systemic human infection. Thus, analysis of the data generated by genomic surveillance systems permits conclusions on the relevance of genes for pathogen biology, ultimately supporting functional annotation of the *L. monocytogenes* genome [75]. Besides this, genomic pathogen surveillance exerted on the global scale helps to reconstruct pathogen transmission routes across countries and allows identification of globally disseminated as well as regionally dominating subtypes [76]. According to our results, the majority of the STs that caused disease in Germany has also been reported from locations abroad. However, numerous subtypes exist that have so far only been found outside Germany while others (e. g. ST173 and ST249) were overrepresented in Germany at the time of analysis. Thus, the population of *L. monocytogenes* subtypes that is pathogenic to humans is composed of internationally widespread clones and subtypes with regionally restricted distribution. Internationally widespread clones can reflect past periods of successful clonal expansion during different phases of globalisation of animal and food trade. One example of this is the worldwide spread of CC1 through the intensification of cattle breeding and the transatlantic livestock trade since the nineteenth century [76].

Conclusions

Taken together, this data set combined with our conclusions provides a comprehensive insight into the population structure of clinical *L. monocytogenes* isolates in Germany and the genetic and clinical characteristics of the most abundant phylogenetic subtypes. The assignment of hyper- and hypovirulent lineages may help to prioritise clusters for epidemiological investigations and to concentrate future work on the identification of the underlying genetic determinants, which might lead to the discovery of relevant virulence factors outside of reference strains.

Supplementary Information

The online version contains supplementary material available at https://doi.org/10.1186/s13073-024-01389-2.

Supplementary Material 1: Fig. S1. Comparison of the population structures of clinical *L. monocytogenes* isolates from in- and outside Germany. Fig. S2. Clinical disease manifestation as reported during case notification for different serogroups. Fig. S3. Duration and geographical spread of listeriosis clusters. Fig. S4. Absence of an Epsilon1b prophage in the *L. monocytogenes* Epsilon1a outbreak clone. Table S1. Clinical *L. monocytogenes* isolates included in this study. Table S2. Genomic features of representative isolates from selected German outbreak clusters. Table S3. Subpopulations of clinical *L. monocytogenes* isolates with inactivating mutations in selected genes.

Acknowledgements
We thank Simone Dumschat and Birgitt Hahn for excellent technical assistance and the Genome Competence Centre of the RKI for sequencing of *L. monocytogenes* genomes. We also would like to thank all the primary diagnostic labs for submission of *L. monocytogenes* strains. We further acknowledge Jeanine Rismondo (University of Göttingen) and Angelika Gründling (Imperial College, London) for sharing strain 10403S and the Δ*esiB* mutant.

Authors' contributions
Study design: SH, HW and AF; data acquisition: SH, SW, RL, AH, AP, WR; data analysis and interpretation: SH, SW, RL; manuscript draft: SH, SW, RL, AF. Editing of the final version: SH, SW, RL, AH, AP, WR, HW, AF. All authors read and approved the final manuscript.

Funding
Open Access funding enabled and organized by Projekt DEAL. This work was funded by DFG grant HA6830/5-1 (to SH) and financing by the German Ministry of Health dedicated to the Consultant Laboratory for *Listeria* (to AF). The funders had no role in the design of the study, collection and analysis of data, decision to publish or preparation of the manuscript.

Availability of data and materials
Strains analysed during the current study are available from the corresponding author on reasonable request. All genome sequencing data are available at the European Nucleotide Archive using the accession numbers given in Supplementary Table S1.

Declarations

Ethics approval and consent to participate
Not applicable.

Consent for publication
Not applicable.

Competing interests
The authors have no conflicts of interest to declare.

Received: 13 February 2024 Accepted: 24 September 2024
Published online: 07 October 2024

References

1. Matle I, Mbatha KR, Madoroba E. A review of *Listeria monocytogenes* from meat and meat products: epidemiology, virulence factors, antimicrobial resistance and diagnosis. Onderstepoort J Vet Res. 2020;87(1):e1–20. https://doi.org/10.4102/ojvr.v87i1.1869.
2. Wilking H, Lachmann R, Holzer A, Halbedel S, Flieger A, Stark K. Ongoing high incidence and case-fatality rates for invasive listeriosis, Germany, 2010–2019. Emerg Infect Dis. 2021;27(9):2485–8. https://doi.org/10.3201/eid2709.210068.
3. Pohl AM, Pouillot R, Bazaco MC, Wolpert BJ, Healy JM, Bruce BB, et al. Differences among incidence rates of invasive listeriosis in the U.S. FoodNet population by age, sex, race/ethnicity, and pregnancy status, 2008–2016. Foodborne Pathog Dis. 2019;16(4):290–7. https://doi.org/10.1089/fpd.2018.2548.
4. Authority EFS, Prevention ECfD, Control. The European Union One Health 2020 zoonoses report. EFSA Journal. 2021;19(12):e06971. https://doi.org/10.2903/j.efsa.2021.6971.
5. Vazquez-Boland JA, Kuhn M, Berche P, Chakraborty T, Dominguez-Bernal G, Goebel W, et al. *Listeria* pathogenesis and molecular virulence determinants. Clin Microbiol Rev. 2001;14(3):584–640. https://doi.org/10.1128/CMR.14.3.584-640.2001.
6. Quereda JJ, Moron-Garcia A, Palacios-Gorba C, Dessaux C, Garcia-Del Portillo F, Pucciarelli MG, et al. Pathogenicity and virulence of *Listeria monocytogenes*: a trip from environmental to medical microbiology. Virulence. 2021;12(1):2509–45. https://doi.org/10.1080/21505594.2021.1975526.
7. Scallan E, Hoekstra RM, Angulo FJ, Tauxe RV, Widdowson MA, Roy SL, et al. Foodborne illness acquired in the United States—major pathogens. Emerg Infect Dis. 2011;17(1):7–15. https://doi.org/10.3201/eid1701.P11101.
8. Charlier C, Perrodeau E, Leclercq A, Cazenave B, Pilmis B, Henry B, et al. Clinical features and prognostic factors of listeriosis: the MONALISA national prospective cohort study. Lancet Infect Dis. 2017;17(5):510–9. https://doi.org/10.1016/S1473-3099(16)30521-7. Epub 20170128.
9. Werber D, Hille K, Frank C, Dehnert M, Altmann D, Müller-Nordhorn J, et al. Years of potential life lost for six major enteric pathogens, Germany, 2004–2008. Epidemiology and infection. 2013;141(5):961–8. https://doi.org/10.1017/S0950268812001550. Epub 2012/07/21.
10. Autio T, Markkula A, Hellstrom S, Niskanen T, Lunden J, Korkeala H. Prevalence and genetic diversity of *Listeria monocytogenes* in the tonsils of pigs. J Food Prot. 2004;67(4):805–8. https://doi.org/10.4315/0362-028x-67.4.805.
11. Hellstrom S, Laukkanen R, Siekkinen KM, Ranta J, Maijala R, Korkeala H. *Listeria monocytogenes* contamination in pork can originate from farms. J Food Prot. 2010;73(4):641–8. https://doi.org/10.4315/0362-028x-73.4.641.
12. Walland J, Lauper J, Frey J, Imhof R, Stephan R, Seuberlich T, et al. *Listeria monocytogenes* infection in ruminants: is there a link to the environment, food and human health? A review Schweiz Arch Tierheilkd. 2015;157(6):319–28. https://doi.org/10.17236/sat00022.
13. Vivant AL, Garmyn D, Piveteau P. *Listeria monocytogenes*, a down-to-earth pathogen. Front Cell Infect Microbiol. 2013;3:87. https://doi.org/10.3389/fcimb.2013.00087.
14. Miceli A, Settanni L. Influence of agronomic practices and pre-harvest conditions on the attachment and development of *Listeria monocytogenes* in vegetables. Annals of Microbiology. 2019;69(3):185–99. https://doi.org/10.1007/s13213-019-1435-6.
15. Mazaheri T, Cervantes-Huaman BRH, Bermudez-Capdevila M, Ripolles-Avila C, Rodriguez-Jerez JJ. *Listeria monocytogenes* biofilms in the food industry: is the current hygiene program sufficient to combat the persistence of the pathogen? Microorganisms. 2021;9(1). https://doi.org/10.3390/microorganisms9010181.
16. Commission Regulation (EC) No 2073/2005 of 15 November 2005 on microbiological criteria for foodstuffs. 2020. https://eur-lex.europa.eu/legal-content/EN/TXT/?uri=CELEX%3A02005R2073-20200308.
17. Thomas J, Govender N, McCarthy KM, Erasmus LK, Doyle TJ, Allam M, et al. Outbreak of listeriosis in South Africa associated with processed meat. N Engl J Med. 2020;382(7):632–43. https://doi.org/10.1056/NEJMoa1907462.
18. Halbedel S, Wilking H, Holzer A, Kleta S, Fischer MA, Luth S, et al. Large nationwide outbreak of invasive listeriosis associated with blood sausage, Germany, 2018–2019. Emerg Infect Dis. 2020;26(7):1456–64. https://doi.org/10.3201/eid2607.200225.
19. Fernandez-Martinez NF, Ruiz-Montero R, Briones E, Banos E, Garcia San Miguel Rodriguez-Alarcon L, Chaves JA, et al. Listeriosis outbreak caused by contaminated stuffed pork, Andalusia, Spain, July to October 2019. Euro Surveill. 2022;27(43). https://doi.org/10.2807/1560-7917.ES.2022.27.43.2200279.
20. Halbedel S, Prager R, Fuchs S, Trost E, Werner G, Flieger A. Whole-genome sequencing of recent *Listeria monocytogenes* isolates from Germany

reveals population structure and disease clusters. J Clin Microbiol. 2018;56(6). https://doi.org/10.1128/JCM.00119-18. Epub 20180525.
21. Moura A, Tourdjman M, Leclercq A, Hamelin E, Laurent E, Fredriksen N, et al. Real-time whole-genome sequencing for surveillance of *Listeria monocytogenes*. France Emerging infectious diseases. 2017;23(9):1462–70. https://doi.org/10.3201/eid2309.170336.
22. Kwong JC, Mercoulia K, Tomita T, Easton M, Li HY, Bulach DM, et al. Prospective whole-genome sequencing enhances national surveillance of *Listeria monocytogenes*. J Clin Microbiol. 2016;54(2):333–42. https://doi.org/10.1128/JCM.02344-15.
23. Van Walle I, Bjorkman JT, Cormican M, Dallman T, Mossong J, Moura A, et al. Retrospective validation of whole genome sequencing-enhanced surveillance of listeriosis in Europe, 2010 to 2015. Euro Surveill. 2018;23(33). https://doi.org/10.2807/1560-7917.ES.2018.23.33.1700798.
24. Jackson BR, Tarr C, Strain E, Jackson KA, Conrad A, Carleton H, et al. Implementation of nationwide real-time whole-genome sequencing to enhance listeriosis outbreak detection and investigation. Clinical infectious diseases : an official publication of the Infectious Diseases Society of America. 2016;63(3):380–6. https://doi.org/10.1093/cid/ciw242.
25. Lachmann R, Halbedel S, Lüth S, Holzer A, Adler M, Pietzka A, et al. Invasive listeriosis outbreaks and salmon products: a genomic, epidemiological study. Emerg Microbes Infect. 2022:1–30. https://doi.org/10.1080/22221751.2022.2063075.
26. Maury MM, Tsai YH, Charlier C, Touchon M, Chenal-Francisque V, Leclercq A, et al. Uncovering *Listeria monocytogenes* hypervirulence by harnessing its biodiversity. Nat Genet. 2016;48(3):308–13. https://doi.org/10.1038/ng.3501.
27. Harter E, Wagner EM, Zaiser A, Halecker S, Wagner M, Rychli K. Stress survival islet 2, predominantly present in *Listeria monocytogenes* strains of sequence type 121, is involved in the alkaline and oxidative stress responses. Appl Environ Microbiol. 2017;83(16). https://doi.org/10.1128/AEM.00827-17.
28. Kremer PH, Lees JA, Koopmans MM, Ferwerda B, Arends AW, Feller MM, et al. Benzalkonium tolerance genes and outcome in *Listeria monocytogenes* meningitis. Clin Microbiol Infect. 2017;23(4):265 e1–e7. https://doi.org/10.1016/j.cmi.2016.12.008.
29. Fischer MA, Wamp S, Fruth A, Allerberger F, Flieger A, Halbedel S. Population structure-guided profiling of antibiotic resistance patterns in clinical *Listeria monocytogenes* isolates from Germany identifies *pbpB3* alleles associated with low levels of cephalosporin resistance. Emerg Microbes Infect. 2020;9(1):1804–13. https://doi.org/10.1080/22221751.2020.1799722.
30. Lüth S, Halbedel S, Rosner B, Wilking H, Holzer A, Roedel A, et al. Backtracking and forward checking of human listeriosis clusters identified a multiclonal outbreak linked to *Listeria monocytogenes* in meat products of a single producer. Emerg Microbes Infect. 2020:1–34. https://doi.org/10.1080/22221751.2020.1784044.
31. Lachmann R, Halbedel S, Adler M, Becker N, Allerberger F, Holzer A, et al. Nationwide outbreak of invasive listeriosis associated with consumption of meat products in health care facilities, Germany, 2014–2019. Clin Microbiol Infect. 2021;27(7):1035 e1–e5. https://doi.org/10.1016/j.cmi.2020.09.020.
32. Ruppitsch W, Prager R, Halbedel S, Hyden P, Pietzka A, Huhulescu S, et al. Ongoing outbreak of invasive listeriosis, Germany, 2012 to 2015. Euro Surveill. 2015;20(50). https://doi.org/10.2807/1560-7917.ES.2015.20.50.30094.
33. Glaser P, Frangeul L, Buchrieser C, Rusniok C, Amend A, Baquero F, et al. Comparative genomics of *Listeria* species. Science. 2001;294(5543):849–52. https://doi.org/10.1126/science.1063447294/5543/849 . Epub 2001/10/27. [pii].
34. Mandin P, Repoila F, Vergassola M, Geissmann T, Cossart P. Identification of new noncoding RNAs in *Listeria monocytogenes* and prediction of mRNA targets. Nucleic Acids Res. 2007;35(3):962–74. https://doi.org/10.1093/nar/gkl1096.
35. Halbedel S, Hahn B, Daniel RA, Flieger A. DivIVA affects secretion of virulence-related autolysins in *Listeria monocytogenes*. Mol Microbiol. 2012;83(4):821–39. https://doi.org/10.1111/j.1365-2958.2012.07969.x. Epub 20120118.
36. Fischer MA, Engelgeh T, Rothe P, Fuchs S, Thürmer A, Halbedel S. *Listeria monocytogenes* genes supporting growth under standard laboratory cultivation conditions and during macrophage infection. Genome Res. 2022;32(9):1711–26. https://doi.org/10.1101/gr.276747.122. Epub 20220916.
37. Rismondo J, Bender JK, Halbedel S. Suppressor mutations linking *gpsB* with the first committed step of peptidoglycan biosynthesis in *Listeria monocytogenes*. J Bacteriol. 2017;199(1). https://doi.org/10.1128/JB.00393-16. Epub 20161213.
38. Rismondo J, Schulz LM, Yacoub M, Wadhawan A, Hoppert M, Dionne MS, et al. EslB is required for cell wall biosynthesis and modification in *Listeria monocytogenes*. J Bacteriol. 2021;203(4). https://doi.org/10.1128/JB.00553-20. Epub 20210125.
39. Köser CU, Fraser LJ, Ioannou A, Becq J, Ellington MJ, Holden MT, et al. Rapid single-colony whole-genome sequencing of bacterial pathogens. The Journal of antimicrobial chemotherapy. 2014;69(5):1275–81. Epub 20131225. https://doi.org/10.1093/jac/dkt494.
40. Ruppitsch W, Pietzka A, Prior K, Bletz S, Fernandez HL, Allerberger F, et al. Defining and evaluating a core genome multilocus sequence typing scheme for whole-genome sequence-based typing of *Listeria monocytogenes*. J Clin Microbiol. 2015;53(9):2869–76. https://doi.org/10.1128/JCM.01193-15.
41. Letunic I, Bork P. Interactive Tree Of Life (iTOL) v5: an online tool for phylogenetic tree display and annotation. Nucleic Acids Res. 2021;49(W1):W293–6. https://doi.org/10.1093/nar/gkab301.
42. Wick R, Menzel P. Filtlong. 2021. Available from: https://github.com/rrwick/Filtlong. Cited 2021 01.07.2021.
43. Wick RR, Judd LM, Gorrie CL, Holt KE. Unicycler: resolving bacterial genome assemblies from short and long sequencing reads. PLoS Comput Biol. 2017;13(6):e1005595. https://doi.org/10.1371/journal.pcbi.1005595.
44. Fischer MA, Thürmer A, Flieger A, Halbedel S. Complete genome sequences of three clinical *Listeria monocytogenes* sequence type 8 strains from recent German listeriosis outbreaks. Microbiol Resour Announc. 2021;10(18). https://doi.org/10.1128/MRA.00303-21.
45. Becker L, Fuchs S, Pfeifer Y, Semmler T, Eckmanns T, Korr G, et al. Whole genome sequence analysis of CTX-M-15 producing *Klebsiella* isolates allowed dissecting a polyclonal outbreak scenario. Frontiers in microbiology. 2018;9(322). https://doi.org/10.3389/fmicb.2018.00322.
46. Vazquez-Boland JA, Wagner M, Scortti M. Why are some *Listeria monocytogenes* genotypes more likely to cause invasive (brain, placental) infection? mBio. 2020;11(6). https://doi.org/10.1128/mBio.03126-20. Epub 20201215.
47. Deeks JJ, Higgins JP, Altman DG, Group obotCSM. Analysing data and undertaking meta-analyses. Cochrane handbook for systematic reviews of interventions 2019. p. 241–84.
48. Abdelhamed H, Lawrence ML, Karsi A. A novel suicide plasmid for efficient gene mutation in *Listeria monocytogenes*. Plasmid. 2015;81:1–8. Epub 20150531. https://doi.org/10.1016/j.plasmid.2015.05.003.
49. Halbedel S, Prager R, Banerji S, Kleta S, Trost E, Nishanth G, et al. A *Listeria monocytogenes* ST2 clone lacking chitinase ChiB from an outbreak of non-invasive gastroenteritis. Emerg Microbes Infect. 2019;8(1):17–28. https://doi.org/10.1080/22221751.2018.1558960.
50. Halbedel S, Reiss S, Hahn B, Albrecht D, Mannala GK, Chakraborty T, et al. A systematic proteomic analysis of *Listeria monocytogenes* housekeeping protein secretion systems. Molecular & cellular proteomics : MCP. 2014;13(11):3063–81. https://doi.org/10.1074/mcp.M114.041327.
51. Dominguez-Bernal G, Muller-Altrock S, Gonzalez-Zorn B, Scortti M, Herrmann P, Monzo HJ, et al. A spontaneous genomic deletion in *Listeria ivanovii* identifies LIPI-2, a species-specific pathogenicity island encoding sphingomyelinase and numerous internalins. Mol Microbiol. 2006;59(2):415–32. https://doi.org/10.1111/j.1365-2958.2005.04955.x.
52. Yin Y, Yao H, Doijad S, Kong S, Shen Y, Cai X, et al. A hybrid sub-lineage of *Listeria monocytogenes* comprising hypervirulent isolates. Nat Commun. 2019;10(1):4283. https://doi.org/10.1038/s41467-019-12072-1.
53. Clayton EM, Daly KM, Guinane CM, Hill C, Cotter PD, Ross PR. Atypical *Listeria innocua* strains possess an intact LIPI-3. BMC Microbiol. 2014;14:58. https://doi.org/10.1186/1471-2180-14-58.
54. Ryan S, Begley M, Hill C, Gahan CG. A five-gene stress survival islet (SSI-1) that contributes to the growth of *Listeria monocytogenes* in suboptimal conditions. J Appl Microbiol. 2010;109(3):984–95. https://doi.org/10.1111/j.1365-2672.2010.04726.x.
55. Lee S, Ward TJ, Jima DD, Parsons C, Kathariou S. The arsenic resistance-associated *Listeria* genomic island LGI2 exhibits sequence and integration

site diversity and a propensity for three *Listeria monocytogenes* clones with enhanced virulence. Appl Environ Microbiol. 2017;83(21). https://doi.org/10.1128/AEM.01189-17.
56. Parsons C, Lee S, Jayeola V, Kathariou S. Novel cadmium resistance determinant in *Listeria monocytogenes*. Appl Environ Microbiol. 2017;83(5). https://doi.org/10.1128/AEM.02580-16.
57. Müller A, Rychli K, Muhterem-Uyar M, Zaiser A, Stessl B, Guinane CM, et al. Tn6188 - a novel transposon in *Listeria monocytogenes* responsible for tolerance to benzalkonium chloride. PLoS One. 2013;8(10):e76835. https://doi.org/10.1371/journal.pone.0076835.
58. Halbedel S, Sperle I, Lachmann R, Kleta S, Fischer MA, Wamp S, et al. Large multicountry outbreak of invasive listeriosis by a *Listeria monocytogenes* ST394 clone linked to smoked rainbow trout, 2020 to 2021. Microbiol Spectr. 2023:e0352022. https://doi.org/10.1128/spectrum.03520-22. Epub 20230410.
59. Palma F, Mangone I, Janowicz A, Moura A, Chiaverini A, Torresi M, et al. In vitro and in silico parameters for precise cgMLST typing of *Listeria monocytogenes*. BMC Genomics. 2022;23(1):235. https://doi.org/10.1186/s12864-022-08437-4. Epub 20220326.
60. Ling Z, Zhao D, Xie X, Yao H, Wang Y, Kong S, et al. *inlF* enhances *Listeria monocytogenes* early-stage infection by inhibiting the inflammatory response. Frontiers in cellular and infection microbiology. 2021;11:748461.https://doi.org/10.3389/fcimb.2021.748461. Epub 20220210.
61. Eugster MR, Haug MC, Huwiler SG, Loessner MJ. The cell wall binding domain of *Listeria* bacteriophage endolysin PlyP35 recognizes terminal GlcNAc residues in cell wall teichoic acid. Mol Microbiol. 2011;81(6):1419–32. https://doi.org/10.1111/j.1365-2958.2011.07774.x.
62. Ragon M, Wirth T, Hollandt F, Lavenir R, Lecuit M, Le Monnier A, et al. A new perspective on *Listeria monocytogenes* evolution. PLoS Pathog. 2008;4(9): e1000146. https://doi.org/10.1371/journal.ppat.1000146.
63. Moura A, Criscuolo A, Pouseele H, Maury MM, Leclercq A, Tarr C, et al. Whole genome-based population biology and epidemiological surveillance of *Listeria monocytogenes*. Nat Microbiol. 2016;2:16185. https://doi.org/10.1038/nmicrobiol.2016.185.
64. Moura A, Lefrancq N, Wirth T, Leclercq A, Borges V, Gilpin B, et al. Emergence and global spread of *Listeria monocytogenes* main clinical clonal complex. Sci Adv. 2021;7(49):9805. https://doi.org/10.1126/sciadv.abj9805. Epub 20211201.
65. Nuesch-Inderbinen M, Bloemberg GV, Muller A, Stevens MJA, Cernela N, Kolloffel B, et al. Listeriosis caused by persistence of *Listeria monocytogenes* serotype 4b sequence type 6 in cheese production environment. Emerg Infect Dis. 2021;27(1):284–8. https://doi.org/10.3201/eid2701.203266.
66. McLauchlin J, Aird H, Amar C, Barker C, Dallman T, Lai S, et al. An outbreak of human listeriosis associated with frozen sweet corn consumption: investigations in the UK. Int J Food Microbiol. 2021;338:108994. https://doi.org/10.1016/j.ijfoodmicro.2020.108994. Epub 20201127.
67. Wagner E, Zaiser A, Leitner R, Quijada NM, Pracser N, Pietzka A, et al. Virulence characterization and comparative genomics of *Listeria monocytogenes* sequence type 155 strains. BMC Genomics. 2020;21(1):847. https://doi.org/10.1186/s12864-020-07263-w. Epub 20201130.
68. Wagner E, Fagerlund A, Thalguter S, Jensen MR, Heir E, Moretro T, et al. Deciphering the virulence potential of *Listeria monocytogenes* in the Norwegian meat and salmon processing industry by combining whole genome sequencing and in vitro data. Int J Food Microbiol. 2022;383:109962. https://doi.org/10.1016/j.ijfoodmicro.2022.109962. Epub 20221008.
69. Papic B, Pate M, Felix B, Kusar D. Genetic diversity of *Listeria monocytogenes* strains in ruminant abortion and rhombencephalitis cases in comparison with the natural environment. BMC Microbiol. 2019;19(1):299. https://doi.org/10.1186/s12866-019-1676-3. Epub 20191218.
70. Cardenas-Alvarez MX, Townsend Ramsett MK, Malekmohammadi S, Bergholz TM. Evidence of hypervirulence in *Listeria monocytogenes* clonal complex 14. J Med Microbiol. 2019;68(11):1677–85. https://doi.org/10.1099/jmm.0.001076.
71. Ghosh P, Halvorsen EM, Ammendolia DA, Mor-Vaknin N, O'Riordan MXD, Brumell JH, et al. Invasion of the brain by *Listeria monocytogenes* is mediated by InlF and host cell vimentin. mBio. 2018;9(1). https://doi.org/10.1128/mBio.00160-18. Epub 20180227.
72. Faralla C, Rizzuto GA, Lowe DE, Kim B, Cooke C, Shiow LR, et al. InlP, a new virulence factor with strong placental tropism. Infect Immun. 2016;84(12):3584–96. https://doi.org/10.1128/IAI.00625-16. Epub 20161118.
73. Balogh D, Eckel K, Fetzer C, Sieber SA. *Listeria monocytogenes* utilizes the ClpP1/2 proteolytic machinery for fine-tuned substrate degradation at elevated temperatures. RSC Chem Biol. 2022;3(7):955–71. https://doi.org/10.1039/d2cb00077f.
74. Elsholz AKW, Birk MS, Charpentier E, Turgay K. Functional diversity of AAA+ protease complexes in *Bacillus subtilis*. Front Mol Biosci. 2017;4:44. https://doi.org/10.3389/fmolb.2017.00044. Epub 20170712.
75. Elfmann C, Zhu B, Stülke J, Halbedel S. *Listi*Wiki: a database for the foodborne pathogen *Listeria monocytogenes*. Int J Med Microbiol. 2023;313(6):151591. https://doi.org/10.1016/j.ijmm.2023.151591. Epub 20231129.
76. Moura A, Lefrancq N, Leclercq A, Wirth T, Borges V, Gilpin B, et al. Emergence and global spread of *Listeria monocytogenes* main clinical clonal complex. bioRxiv. 2020:2020.12.18.423387. https://doi.org/10.1101/2020.12.18.423387.

Publisher's Note